



DESIGN SPECTRUM-BASED SCALING AND PARAMETRIC STUDY OF STRENGTH REDUCTION FACTOR SPECTRUM

D. Karmakar¹ and V. K. Gupta²

ABSTRACT

Strength reduction factors (SRFs) continue to play a key role in obtaining inelastic spectra from the elastic design spectra for the ductility-based earthquake-resistant design. This study proposes a new model to estimate the SRF spectrum in terms of a pseudo-spectral acceleration spectrum and ductility demand ratio with the help of two coefficients. The proposed model is illustrated for an elasto-plastic oscillator in case of five recorded accelerograms and three ductility ratios. The model is used to carry out a parametric study for the explicit dependence of SRF spectrum on strong motion duration, earthquake magnitude, site conditions, and epicentral distance. It is shown that there is no clear and significant dependence of SRF spectrum on strong motion duration, while the dependence on earthquake magnitude, site conditions, and epicentral distance conforms to the trends reported by earlier investigations. In particular, it is confirmed that the dependence of SRF spectrum on earthquake magnitude cannot be ignored.

Introduction

It is considered convenient to characterize seismic hazard at a site via elastic design spectra and to obtain the inelastic design spectrum, for the ductility-based design of structures, as the scaled-down form of an elastic design spectrum. The parameter used for this purpose is called as response modification factor, of which strength reduction factor (SRF) is the key component. SRF takes into account the nonlinear characteristics of the structure and is also responsible for much of the parametric dependence of the response modification factor on various structural and ground motion parameters.

SRF has been the topic of several investigations after Newmark (1973) proposed its analytical estimates for long-period, short-period and zero-period structures as functions of ductility (demand) ratio. Most of these (e.g., Elghadamsi 1987, Miranda 1993) studied the dependence of SRF spectrum (showing the variation of SRF with the initial time-period of the oscillator for a given ductility demand ratio) on ground motion parameters like earthquake magnitude, epicentral distance, local site conditions, and strong motion duration without

¹Formerly Graduate Student, Dept. of Civil Engineering, IIT Kanpur, Kanpur 208016, India

²Professor, Dept. of Civil Engineering, IIT Kanpur, Kanpur 208016, India

properly isolating the effects of the governing parameter from those of the other parameters. Tiwari (2000) and Chakraborti (2005) addressed this limitation by proposing scaling models for SRF spectrum in terms of earthquake magnitude, strong motion duration, predominant period of ground motion, geological site conditions and ductility demand ratio. Their conclusions however need to be examined more directly due to their possible dependence on the model chosen.

A parametric study is carried out here with respect to strong-motion duration, earthquake magnitude, site conditions and epicentral distance in case of elasto-plastic oscillators (with no degradations) with three levels of ductility. Effects of each parameter are studied by considering different ensembles of accelerograms that exhibit the desired (ensemble-to-ensemble) variation in the chosen parameter while the other parameters are held constant. Each ensemble is obtained by modifying accelerograms recorded in the western U.S.A. to match the (pseudo-acceleration) response spectra for a given combination of earthquake magnitude, site conditions, epicentral distance, and focal depth. For a compact presentation of the results in case of each ensemble, a new model is proposed to estimate the SRF spectrum in terms of the normalized pseudo-spectral acceleration (PSA) spectrum for a given ductility ratio. The previous model of this type by Ordaz (1998) used peak ground displacement as an input parameter, which may not be always convenient for practical application.

Proposed Model

SRF spectrum $R_\mu(T)$ describes the variation of SRF with the initial period T of a nonlinear single-degree-of-freedom oscillator. SRF is defined as the ratio of elastic strength demand to inelastic strength demand such that the displacement ductility ratio is limited to a maximum value of μ , where ductility ratio μ is the ratio of the maximum inelastic displacement of the oscillator to its yield displacement. It is well known that as T approaches 0, $R_\mu(T) \rightarrow 1$, and as T approaches infinity, $R_\mu(T) \rightarrow \mu$. Further, $R_\mu(T)$ is a function of the type of nonlinearity in the oscillator for a given damping and ductility ratio of the oscillator, and earthquake ground motion.

Considering similarities between the PSA response spectrum, $PSA(T)$, normalized by the peak ground acceleration PGA , and the SRF spectrum at short and intermediate time periods, it is proposed to consider following functional dependence of the SRF spectrum on the PSA spectrum:

$$R_\mu(T) = \left(\frac{PSA(T)}{PGA} \right)^\alpha + \mu(1 - e^{-\beta T}) \quad (1)$$

where α and β are the coefficients determined for a ductility (demand) ratio μ and ground motion, such that the total squared error e , defined as

$$e = \sum_{j=1}^M (R_{\mu,j} - \hat{R}_{\mu,j})^2 \quad (2)$$

is minimized. Here, $R_{\mu,j}$ and $\hat{R}_{\mu,j}$ are, respectively, the actual values and the estimated values of $R_{\mu}(T)$ (with the help of Eq. 1) at the j th initial time period of the oscillator. M is the number of periods at which the actual and estimated SRF values are computed. It may be observed that as T tends to infinity, the first term on the right hand side of Eq. 1 tends to zero, while the second term tends to μ .

An elasto-plastic oscillator is used for the numerical illustration. The damping is assumed to be F-damping (i.e., with no effect of nonlinear behaviour) with value equal to 5% of critical damping. Fourth order Runge-Kutta method with an adaptive step size control scheme (with maximum step size, $\Delta t = 0.004$ sec) is used to carry out the nonlinear time-history analysis. SRF spectrum is calculated at ($M =$) 31 initial time periods, $T = 0.01, 0.013, 0.016, 0.02, 0.025, 0.032, 0.04, 0.05, 0.063, 0.079, 0.1, 0.126, 0.158, 0.2, 0.251, 0.316, 0.398, 0.501, 0.631, 0.794, 1.0, 1.259, 1.585, 1.995, 2.512, 3.162, 3.981, 5.012, 6.31, 7.943$ and 10.0 sec.

Table 1. Particulars of earthquake records for illustration of proposed SRF model.

Record No.	Earthquake	Site	Component
1	Eureka, 1954	Eureka Federal Building, Eureka	N79E
2	Coalinga, 1983	Parkfield Fault Zone 9, Parkfield	North
3	Northern California, 1962	Eureka Federal Building, Eureka	N45W
4	San Fernando, 1971	6074 Park Drive, Wrightwood	N25E
5	Coyote Lake, 1979	Gavilan College, Water Tower, Gilroy	S50W

Table 2. α and β values for different earthquake records in case of $\mu = 2, 4$ and 6.

Record No.	$\mu = 2$		$\mu = 4$		$\mu = 6$	
	α	β	α	β	α	β
1	0.5520	0.7144	1.1040	1.1280	1.3860	0.9776
2	0.3960	0.6392	0.2580	1.0528	0.0420	1.0904
3	0.6300	0.1504	0.9360	0.3760	1.0920	0.6392
4	0.4380	1.8800	0.9300	1.7296	1.2720	1.5040
5	0.2880	1.5040	0.6840	3.7600	0.9300	3.3840

The SRF spectra predicted by the proposed model are compared with the actual spectra by considering 5 different recorded accelerograms and $\mu = 2, 4$ and 6. The example accelerograms are listed in Table 1. Table 2 shows the estimated parameters of the proposed model for each of the 15 cases considered here. Fig. 1 shows the comparison for $\mu = 4$ in case

of Coalinga Earthquake ground motion (Record No. 2). From this and many such figures, it is concluded that the proposed model captures the behaviour of SRF spectrum reasonably well, particularly for periods up to 1.0 sec, even though it does not exactly capture the peaks in SRF spectrum at different time periods. Considering that most structural systems lie in the period range of 0.1 to 2 sec, the proposed model may be deemed satisfactory for practical applications.

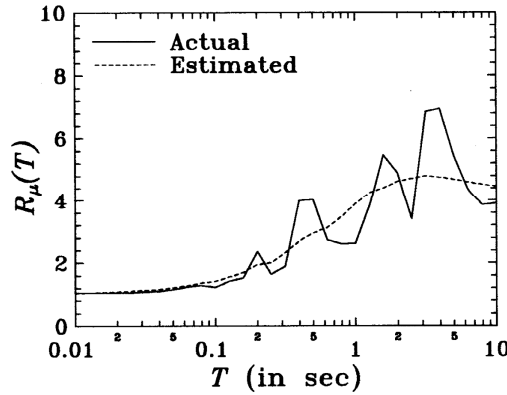


Figure 1. Comparison of actual and estimated SRF spectra for $\mu = 4$ in case of Coalinga earthquake motion (record no. 2).

A more stable estimation of the parameters, α and β , may be carried out by minimizing the total squared error e over an ensemble of N accelerograms rather than over just one accelerogram. This however requires the availability of accelerograms that are compatible with the same PSA spectrum. This option is illustrated next in the parametric study on SRF spectrum.

Parametric Study

In order to study the effects of different ground motion parameters like strong motion duration, earthquake magnitude, site conditions, and epicentral distance on the SRF spectrum, different ensembles of accelerograms compatible with different PSA spectra have been obtained. The wavelet-based procedure of Mukherjee (2002) has been used to generate the synthetic accelerograms. The synthetic accelerograms so obtained have been passed through a hipass filter, and then baseline correction has been applied to the filtered accelerograms in order to obtain realistic estimates of the nonlinear response. The hipass filter used is Ormsby filter, with the cutoff central frequency of the transition band as 0.06 Hz and the width of the transition band as 0.02 Hz, and the quadratic-type baseline correction has been used. The corrected synthetic accelerograms have been used to get SRF spectra for the following 56 initial time periods: 0.1, 0.11, 0.12, 0.13, 0.14, 0.15, 0.16, 0.17, 0.18, 0.19, 0.20, 0.22, 0.24, 0.26, 0.28, 0.30, 0.32, 0.34, 0.36, 0.38, 0.40, 0.42, 0.44, 0.46, 0.48, 0.50, 0.55, 0.60, 0.65, 0.70, 0.75, 0.80, 0.85, 0.90, 0.95, 1.0, 1.1, 1.2, 1.3, 1.4, 1.5, 1.6, 1.7, 1.8, 1.9, 2.0, 2.2, 2.4, 2.6, 2.8, 3.0, 3.2, 3.4, 3.6, 3.8, 4.0 sec.

The recorded accelerograms used to obtain the ensembles of synthetic accelerograms are from a database of 1274 accelerograms that includes (i) 956 accelerograms recorded during the 106 earthquake events in the western U.S.A. region from 1931 to 1984 (Lee 1987), and (ii) 318 accelerograms recorded during the 1994 Northridge earthquake. The target spectra $PSA(T)$

considered to examine the parametric dependence of SRF spectrum are obtained from the 50%-confidence level, 5% damping pseudo-spectral velocity spectra proposed by Trifunac and Lee (1985) for the western U.S.A. region. These spectra have parametric dependence on earthquake magnitude, epicentral distance, site conditions, and focal depth, and are deemed to be adequate for the parametric study. These however do not consider the strong motion duration as a parameter. In view of this and the fact that the synthetic accelerograms obtained from different recorded accelerograms, but compatible with the same PSA spectrum, have widely different nonstationary characteristics and strong motion durations, parametric dependence on strong motion duration is studied first.

Dependence on Strong Motion Duration

Previous parametric studies involving duration were based on the Trifunac-Brady definition (Trifunac and Brady 1975) for the strong motion duration T_s . Since this definition is based on fixed percentages of energy arrival before and during the strong motion phase, and therefore does not always give realistic estimates of the strong motion duration (Bommer 1999), a generalization of the Trifunac-Brady definition, proposed by Karmakar (2004) and explained in the Appendix, is considered for the parametric study here.

In order to study the dependence of SRF spectrum on T_s , 1274 synthetic accelerograms have been generated (from the 1274 recorded accelerograms) such that those are compatible with the PSA spectrum for earthquake magnitude, $M = 6.5$, epicentral distance, $R = 50$ km, focal depth, $H = 5$ km, and alluvium site conditions. Strong motion duration has been calculated for each of these accelerograms, and then 60 accelerograms for each of the four T_s intervals, i.e. 9.44-10.68, 18.98-20.88, 29.10-31.12, and 38.20-41.60 sec, corresponding respectively to the central T_s values of 10, 20, 30 and 40 sec, have been identified. SRF spectra for these accelerograms have been calculated in the case of elasto-plastic oscillators with $\mu = 4$, and then mean $R_\mu(T)$ spectrum has been obtained for each of the four groups.

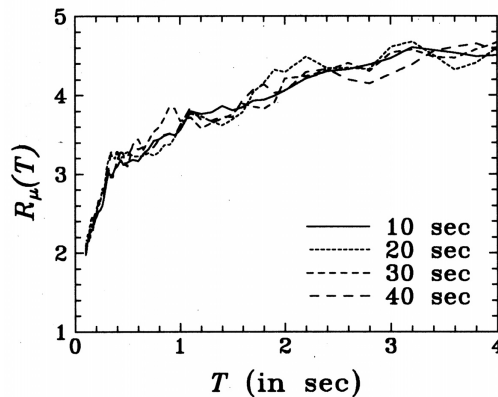


Figure 2. Mean SRF spectra for different central strong motion durations in case of $\mu = 4$.

Fig. 2 shows the comparison of the mean $R_\mu(T)$ spectra for the central T_s values of 10,

20, 30 and 40 sec, respectively. Even though duration seems to make some difference to the SRF spectra in this figure, this difference is nominal and devoid of any clear trend. All four curves seem to crisscross each other randomly within a narrow band of SRF values. Table 3 shows the coefficients, α and β , of the proposed SRF spectrum model corresponding to each of the central T_s values. It may be observed that both parameters of the proposed model exhibit little variations with respect to the T_s values. In view of this, the dependence of SRF spectrum on strong motion duration may be ignored in case of the elasto-plastic oscillators.

Table 3. Coefficients of proposed SRF model for different central values of T_s .

T_s (sec)	α	β
10	1.0140	1.0320
20	1.0860	1.0696
30	1.0620	1.0696
40	1.1280	1.0696

In the following, the dependence of SRF spectrum on other parameters like earthquake magnitude, site conditions and epicentral distance will be studied without giving any weightage to the strong motion duration and thus by treating all synthetic accelerograms alike irrespective of their strong motion durations. This will involve the generation of synthetic accelerograms for several spectral shapes corresponding to different sets of governing parameters. In order to reduce the computational effort in each of these runs, a smaller subset of the database consisting of 474 recorded accelerograms from 72 earthquakes has been chosen such that there is no bias in the chosen data in terms of different ground motion parameters (Karmakar 2004).

Dependence on Earthquake Magnitude, Site Conditions and Epicentral Distance

The values of α and β have been computed for 21 combinations of seven $PSA(T)$ curves and $\mu = 2, 4, 6$. Three out of the seven $PSA(T)$ curves (Spectrum I, Spectrum II, and Spectrum III) correspond to $M = 4.5, 5.5$ and 6.5 , respectively, with $R = 50$ km, $H = 5$ km, and hard rock site conditions. Two curves (Spectrum IV and Spectrum V) correspond to alluvium and intermediate site conditions, respectively, with $R = 50$ km, $H = 5$ km, and $M = 6.5$, while the remaining two (Spectrum VI and Spectrum VII) correspond to $R = 75$ and 100 km, respectively, with $M = 6.5$ km, $H = 5$ km, and hard rock site conditions.

Table 4 shows the values of α and β for all 21 combinations of PSA spectra (Spectra I, II, III, IV, V, VI and VII) and ductility ratios (2, 4 and 6). The use of any of these pairs of α and β in Eq. 1 gives the least-square estimates of SRF spectrum, which should then be combined with the suitable values of (period-dependent) error residuals in order to obtain probabilistic estimates for a given level of confidence. These residuals are found to be log-normally distributed with parameters as given in Karmakar (2004).

Table 4. Coefficients of proposed SRF model for different PSA spectra and ductility ratios.

PSA Spectrum	$\mu = 2$		$\mu = 4$		$\mu = 6$	
	α	β	α	B	α	β
Spectrum I	0.5640	1.1072	0.9060	1.7088	1.1400	1.5584
Spectrum II	0.6120	0.9192	0.9840	1.3704	1.2360	1.2576
Spectrum III	0.7980	1.0696	1.2300	1.4832	1.5540	1.3704
Spectrum IV	0.7440	0.6560	1.1040	0.9568	1.2720	0.9568
Spectrum V	0.7860	0.8440	1.1700	1.2200	1.4400	1.1448
Spectrum VI	0.5760	0.6184	0.8460	1.0320	0.9960	1.0320
Spectrum VII	0.4620	0.5056	0.6840	0.8816	0.8160	0.8816

In order to study the dependence of SRF spectrum on earthquake magnitude, the results in the first three rows of Table 4 (for Spectra I, II and III) are compared. It may be observed that the values of α increase with earthquake magnitude, with a steeper increase in case of higher magnitudes. The values of β decrease significantly from $M = 4.5$ to 5.5 and then increase moderately from $M = 5.5$ to 6.5. Fig. 3 shows the comparison of the $R_\mu(T)$ spectra obtained for Spectra I, II and III by using the α and β values for $\mu = 4$ and error estimates for 50% confidence level. It is observed that lower magnitudes give higher values of SRF for short to medium period range ($T < 1.0$ sec), while higher magnitudes give higher values of SRF for long period range ($T > 1.0$ sec). The effect of earthquake magnitude is particularly significant for the periods longer than 2 sec. These findings are in very good agreement with those reported by Tiwari (2000), and in complete contradiction with those of Miranda (1993).

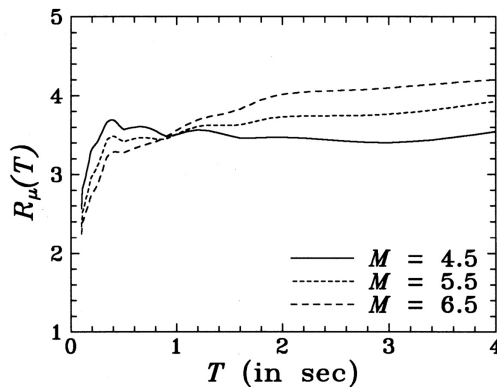


Figure 3. Estimated SRF spectra for different earthquake magnitudes in case of hard rock site, $R = 50$ km, $H = 5$ km, $\mu = 4$, and 50% confidence level.

A comparison of the α and β values in the 3rd, 4th and 5th rows of Table 4 (for Spectra

III, IV and V) shows that both parameters increase as we go from alluvium site conditions to intermediate site conditions and then to hard rock conditions. A comparison of the $R_\mu(T)$ spectra obtained from these values for $\mu = 4$ and 50% confidence level is shown in Fig. 4. It may be observed that except for long periods ($T > 2.5$ sec), hard rock conditions are associated with greater SRF values. However, the effect of site conditions is not as strong as was observed in the case of earthquake magnitude. These results are in agreement with those of Chakraborti (2005) for very long periods ($T > 3$ sec), with those of Tiwari (2000) for short to medium periods ($T < 0.8$ sec), and with those of Elghadamsi (1987) for a large range of periods ($T < 2.5$ sec).

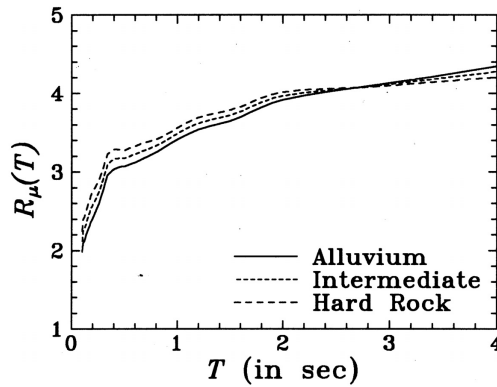


Figure 4. Estimated SRF spectra for different site conditions in case of $M = 6.5$, $R = 50$ km, $H = 5$ km, $\mu = 4$, and 50% confidence level.

The effects of epicentral distance on α and β may be seen in Table 4 by comparing the 3rd, 6th and 7th rows (for Spectra III, VI and VII). Both parameters decrease with an increase in the epicentral distance. However, this does not lead to an appreciable effect of epicentral distance on the SRF spectrum, as shown by Fig. 5 in case of $\mu = 4$ and 50% confidence level. This confirms the observations of Miranda (1993) and others that the effects of epicentral distance on SRF spectrum may be neglected completely.

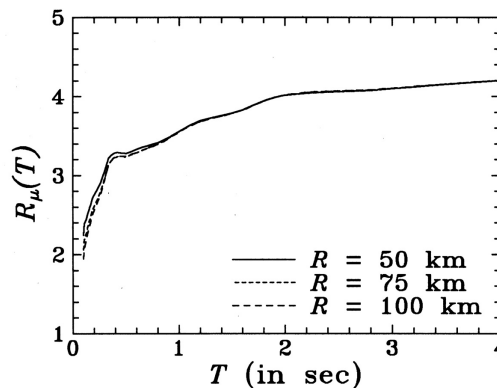


Figure 5. Estimated SRF spectra for different epicentral distances in case of $M = 6.5$, hard rock site, $H = 5$ km, $\mu = 4$, and 50% confidence level.

Conclusions

A new model has been proposed for estimating SRF spectrum in terms of PSA spectrum normalized with respect to peak ground acceleration, and ductility demand ratio. The proposed model is based on two parameters, which are determined based on least-square error matching with the actual SRF spectrum. It has been found through several examples that the performance of the proposed model is good, particularly for periods up to 1.0 sec. The proposed model is convenient for application as it is based on commonly used seismic hazard parameters.

A parametric study has been carried out to study the explicit dependence of SRF spectrum on strong motion duration, earthquake magnitude, site conditions, and epicentral distance in case of elasto-plastic oscillators without degradations. It has been shown that the dependence of SRF spectrum on strong motion duration may be ignored. Further, SRF spectrum depends significantly on earthquake magnitude, particularly for the periods larger than 2 sec. It has been shown that higher magnitude earthquakes are associated with lower values of SRFs in the short to medium period range ($T < 1.0$ sec), and with higher values of SRFs in the long period range ($T > 1.0$ sec). The effect of site conditions is not found to be as strong, and except for very long periods ($T > 2.5$ sec), hard rock conditions are found to be associated with greater SRF values. There is also no appreciable effect of the epicentral distance on the SRF spectrum.

Appendix

The definition of strong motion duration by Karmakar (2004) is a 'significant duration' definition (Bommer 1999), defined as $T_s = T_2 - T_1$, where T_1 and T_2 respectively are the initial and final cut-off times corresponding to certain percentages of the total energy arrival in the accelerogram. Those correspond to $E_n(t) = E_1$ and E_2 respectively, where $E_n(t)$ is the normalized energy level at time t , defined as

$$E_n(t) = \frac{\int_0^t x^2(t)dt}{\int_0^T x^2(t)dt} \quad (3)$$

with $x(t)$ denoting the time-history, and T denoting the total duration of the time-history. The strong motion duration by Trifunac and Brady (1975) is based on the fixed values, $E_1 = 0.05$ and $E_2 = 0.95$.

Karmakar (2004) proposed to make E_1 and E_2 variable for an accelerogram such that the total energy $\Delta E (= E_2 - E_1)$ associated with the strong motion phase arrives in the minimum time and that this (maximum) rate of energy arrival is stationary around the chosen value of ΔE . In the first step, several values of ΔE are considered, and then that value of T_s is considered for each of the ΔE values, which minimizes $T_s (= T_2 - T_1)$ by a suitable choice of E_1 . Through this step, the strong motion segment of the accelerogram is identified for a given ΔE . In the second

step, the largest value of ΔE , say $(\Delta E)_{\text{stationary}}$, that is associated with a stationary rate of energy arrival with respect to the neighbouring lower ΔE values is identified. This is done by calculating the average rate of energy arrival, i.e. $\Delta E/T_s$, at every value of ΔE with reference to the window, $(\Delta E - 0.05, \Delta E)$, and by plotting the average deviation squared with respect to the average value with ΔE . The largest value of ΔE at which a local minimum occurs is taken as $(\Delta E)_{\text{stationary}}$, and the value of T_s corresponding to this value of ΔE in the first step is taken as the strong motion duration.

References

- Bommer, J. J., and A. Martínez-Pereira, 1999. The effective duration of earthquake strong motion, *Journal of Earthquake Engineering* 3 (2), 127-172.
- Chakraborti, A., and V. K. Gupta, 2005. Scaling of strength reduction factors for degrading elasto-plastic oscillators, *Earthquake Engineering and Structural Dynamics* 34, 189-206.
- Elghadamsi, F. E., and B. Mohraz, 1987. Inelastic earthquake spectra, *Earthquake Engineering and Structural Dynamics* 15, 91-104.
- Karmakar, D., 2004. Design spectrum-based scaling of strength reduction factors, *M.Tech. Thesis*, Indian Institute of Technology Kanpur, Kanpur, India.
- Lee, V. W., and M. D. Trifunac, 1987. Strong earthquake ground motion data in EQUINFOS: Part 1, *Report No. CE 87-01*, University of Southern California, Los Angeles.
- Miranda, E., 1993. Site-dependent strength reduction factors, *ASCE Journal of Structural Engineering* 119 (12), 3503-3519.
- Mukherjee, S., and V. K. Gupta, 2002. Wavelet-based generation of spectrum-compatible time-histories, *Soil Dynamics and Earthquake Engineering* 22, 799-804.
- Newmark, N. M., and W. J. Hall, 1973. Procedures and criteria for earthquake resistant design, *Building Practices for Disaster Mitigation* 1, Building Science Series 46, National Bureau of Standards, United States Department of Commerce, Washington, D.C., 209-236.
- Ordaz, M., and L. E. Pérez-Rocha, 1998. Estimation of strength-reduction factors for elastoplastic systems: a new approach, *Earthquake Engineering and Structural Dynamics* 27, 889-901.
- Tiwari, A. K., and V. K. Gupta, 2000. Scaling of ductility and damage-based strength reduction factors for horizontal motions, *Earthquake Engineering and Structural Dynamics* 29, 969-987.
- Trifunac, M. D., and A. G. Brady, 1975. A study of the duration of strong earthquake ground motion, *Bulletin of Seismological Society of America* 65, 581-626.
- Trifunac, M. D., and V. W. Lee, 1985. Preliminary empirical models for scaling pseudo relative velocity spectra of strong earthquake accelerations in terms of magnitude, distance, site intensity and recording site conditions, *Report No. CE 85-04*, University of Southern California, Los Angeles.